

# Hardware Implementation of Chipless RFID Reader and Tags for Moving Targets Identification and Tracking

Yousef Ahmed Abd-Elwahab<sup>a</sup>, Abd-Elrahman Ahmed Abd-Elwahab<sup>b</sup>,  
Mohamed Ibrahim Elhadary<sup>c</sup>, Amr Hussein Hussein<sup>d\*</sup>

<sup>a,b</sup>*Elshaheed Said Abu Azzam School, West Tanta Educational Administration, Fisha Selim Village, Gharbia Governorate, Egypt*

<sup>c</sup>*Tanta University, Faculty of Engineering, Mechanical Power Engineering Dept., Tanta, Egypt*

<sup>d</sup>*Tanta University, Faculty of Engineering, Electronics and Electrical Communications Engineering Dept., Tanta, Egypt*

<sup>a</sup>*Email: Youssef\_daim@yahoo.com*

<sup>b</sup>*Email: Abdo\_daim12@yahoo.com*

<sup>c</sup>*Email: mohamed.elhadary@f-eng.tanta.edu.eg*

<sup>d</sup>*Email: amrvips@yahoo.com and amr.abdallah@f-eng.edu.tanta.eg*

## Abstract

Radio Frequency Identification (RFID) is a rapidly growing technology with significant security implications for humans and military ambushes. In this paper, the hardware implementation of a chipless RFID system using highly efficient Texas instrumentation components is introduced. We introduced the hardware implementation of both RFID reader and 5-bits chipless tags. The proposed reader system is equipped with an ultra-wideband (UWB) radio frequency (RF) power detector that allows the reader to read different types of tags with different code lengths over the frequency range from 10MHz to 8GHz. The proposed spiral resonators based RFID tags are fabricated using microstrip technology on a cheap FR4 lossy substrate with a dielectric constant of  $\epsilon_r = 4.3$ , loss tangent  $\tan \delta = 0.025$ , and thickness  $h = 1.6 \text{ mm}$ . The tags are designed using the computer simulation technology (CST) microwave studio software package. Fortunately, it is found that the experimental measurements of the scattering parameters of the fabricated tags are highly matched to the simulation results.

**Keywords:** Chipless Tags; Radio Frequency Identification (RFID); RF Power Detector.

---

\* Corresponding author.

## 1. Introduction

Radio frequency identification (RFID) is a technology for remote identification of data using electromagnetic waves. The RFID system consists of two main parts, which are the RFID tag, which carries the encrypted data and the RFID reader to receive and decrypt the data. The cost of the system is based on the IC cost of the tag containing the memory chip to store the encrypted information, where the tags with the microchip are more expensive than the chipless or chip-free tags. Recently, there has been a lot of research around the world to design and implement chipless RFID tags, as it appears to be a promising solution. Each RFID chipless tag contains passive resonance circuits that reflect back electromagnetic waves (EMW) to the RFID reader. These resonance circuits encode the frequency spectrum of the incident EMWs in the form of amplitude attenuations at the resonance frequencies of the existing resonance circuits. At the reader, the data is decoded from the reflected radio waves where the presence of amplitude attenuation represents a logic "1" and the absence of amplitude attenuation represents a logic "0".

Various techniques for implementing chipless RFID tags on a frequency basis have been presented in [1-6]. In [1], single-band resonators are presented where each resonator encodes only one data bit. The main disadvantage of this technique is that it provides large size tags [1]. Dual band resonators have been introduced in [2, 3] for efficient utilization of the available tag space. In [2], the incorporation of the stub-loaded dual-band resonators into the frequency encoded chipless RFID tags has been introduced. This technique allows the encoding of  $3^N$  words in a single tag when using  $N$  dual-band resonators. Also, it provided significant bandwidth improvement compared to the use of the conventional half-wave resonators. In [3], a modified complementary split-ring resonators (MCSRR) have been introduced to independently encode two data bits instead of one bit. Therefore, for  $N$  MCSRRs the resultant tag is capable of encoding  $4^N$  words. The MCSRR saves 56% of the occupied area compared with the two separate rings based complementary split ring resonators (CSRR). Moreover, the MCSRR reduces the resonance bandwidth by more than 60%. In [4], a passive microstrip chipless RFID system based on the integration of spiral multi-resonator circuit and cross-polarized transmitting and receiving ultra-wideband (UWB) monopole antenna is introduced. The data is encoded in the tag using both the amplitude and phase of the spectral signature of the multi-resonator circuit. It is succeeded to introduce a 35-bits chipless RFID tag for low-cost implementation. In [5], a novel circular patch multiple slot ring resonators based design of a printable small size and orientation independent chipless RFID tag is introduced. This symmetric geometry of the tag has the advantage to be read from any orientation with the reader antennas. The same concept of multiple circular ring patch resonators has been used in [6] where a 19-bits tag has been implemented within a compact surface of 1 cm. In [7], chipless RFID tags using multiple microstrip open stub resonators have been presented. These tags suffer from non-uniform spacing between the successive resonances.

In [8], the design of an automated parking system using RFID technology was introduced. It can be used to manage and monitor various reports and parking system operations. Using this program, the check-in and check-out will be controlled by RFID tags, RFID readers and barriers. Drivers will not have to wait for their cars to be recognized, as this will be done automatically through the signs provided to them. This will also ensure security as only registered users are allowed in. In [9], an RFID-based vehicle localization method for Intelligent

Transportation Systems (ITS) was introduced. UHF RFID tag is used as electronic license and applied to vehicle windshield. The RFID readers and antennas are installed on traffic signal poles on the roads. The phase difference in the arrival of the RFID backscattering signal is used to estimate the distances between the tag and the antennas.

In this paper, the hardware implementation of both chipless RFID reader and 5-bits chipless tags are introduced. The proposed reader system is equipped with a high sensitivity wide band RF power detector that allows the system to work over a wide range of frequencies from 10MHz to 8GHz. Thereby, the proposed RFID reader will be able to read wide varieties of chipless tags with different code lengths. The tags are fabricated using microstrip technology using FR4 (lossy) substrate with  $\epsilon_r = 4.3$ ,  $h = 1.6 \text{ mm}$ , and  $\delta = 0.025$ .

## 2. Practical Implementation Of The Proposed RFID Reader System

In this section, the hardware implementation of a proposed chipless RFID reader system is introduced. The block diagram of the proposed system is shown in Fig. 1. While the practical implementations of the proposed RFID reader transmitter and receiver are shown in Fig. 2 and Fig. 3, respectively. The basic building blocks of the proposed RFID reader system can be divided into four blocks as follows:

1. RFID reader transmitter.
2. RFID reader receiver.
3. Control unit and monitoring system.
4. RFID Reader TX/RX Horn Antennas.

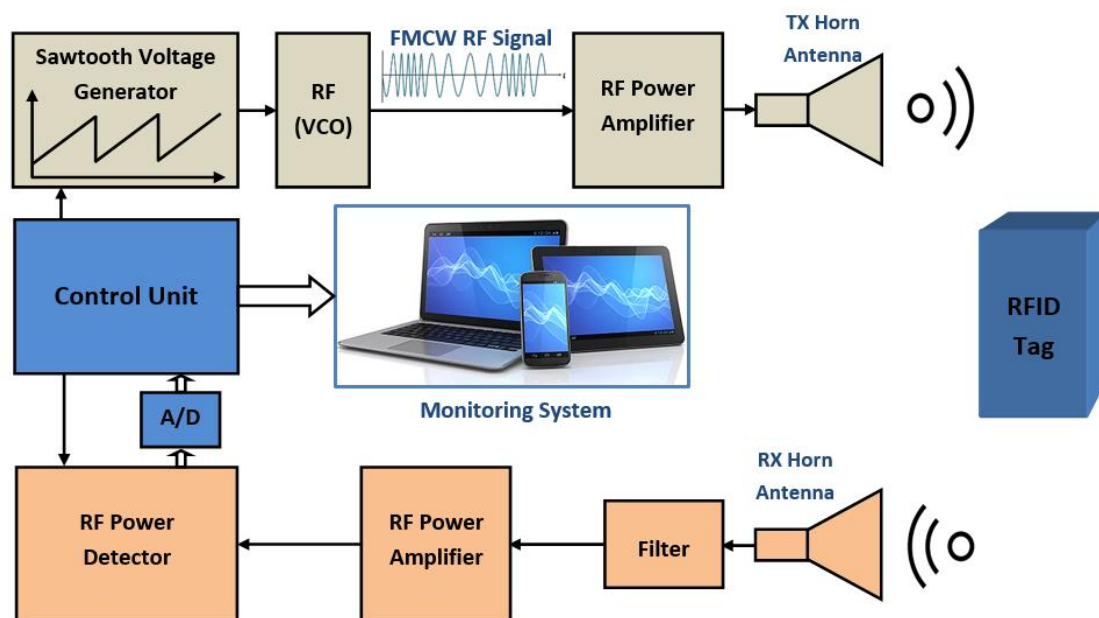


Figure 1: Block diagram of the proposed RFID reader system.

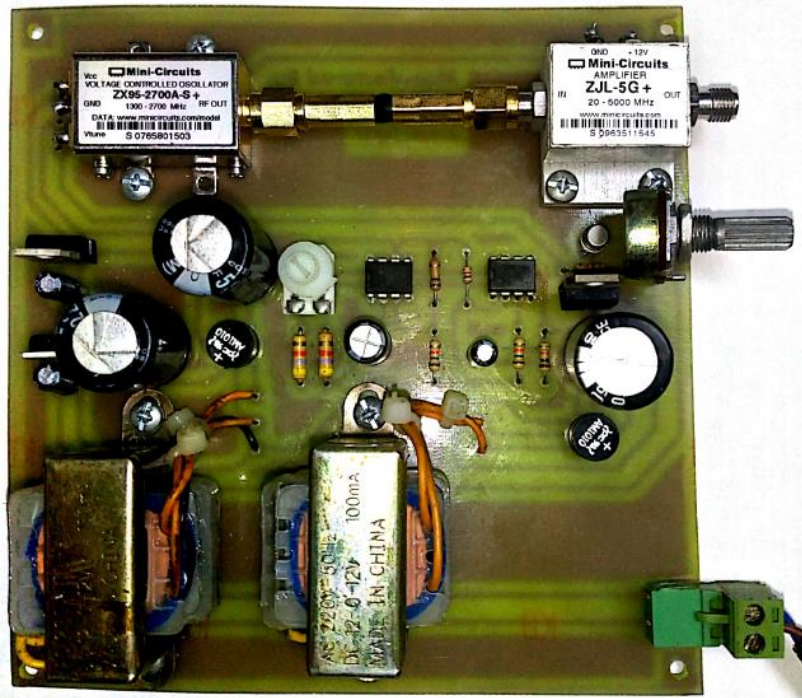


Figure 2: Hardware implementation of the proposed RFID reader transmitting system.

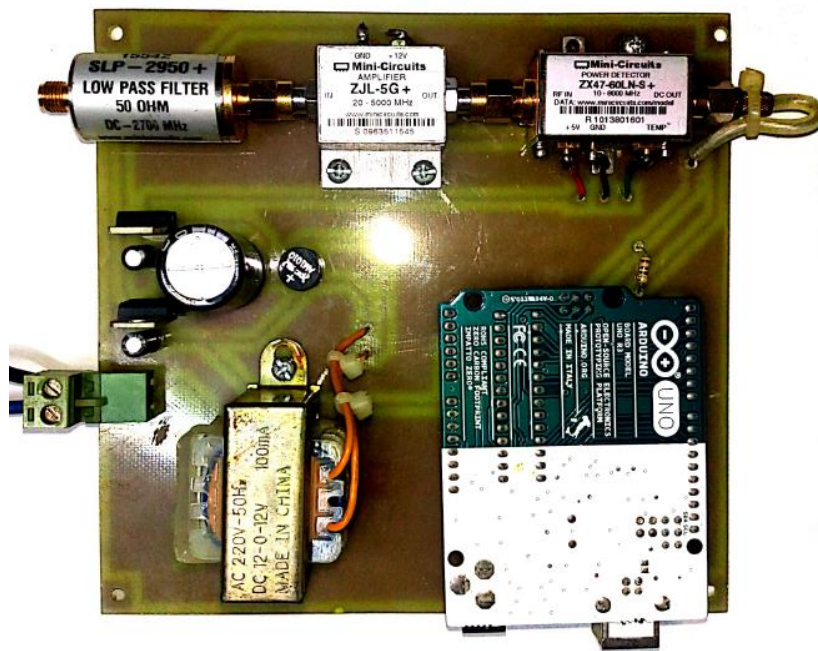
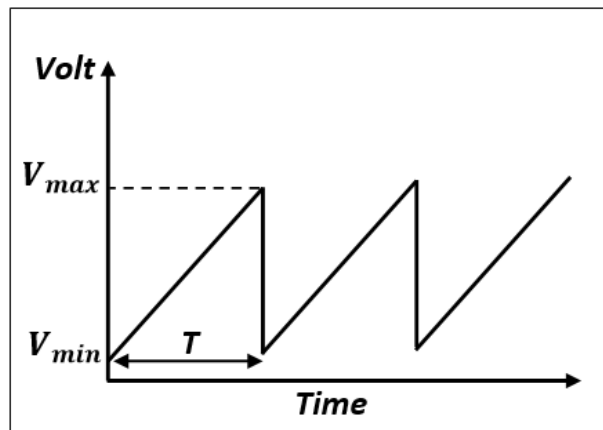


Figure 3: Hardware implementation of the proposed RFID reader receiving system.

## 2.1 RFID Reader Transmitter

The transmitter consists of four elements i.e. the sawtooth voltage generator, RF voltage controlled oscillator (VCO), RF power amplifier, and the transmit horn antenna. The main idea of the transmitter is based on generating a constant amplitude 1300-2700 MHz frequency modulated continuous wave (FMCW) that is

amplified before it is fed to the TX antenna. When the radiated FMCW falls on an N-bits RFID tag having  $N$  number of resonances, the FMCW amplitude will be modulated at these resonance frequencies before it is reflected back to the RX antenna. The basic building block of the reader transmitter is the (ZX95-2700A+) VCO. It provides RF signal with output power  $3.3\text{ dBm}$  and tuning voltage from  $0.15\text{ V}$  to  $25\text{ V}$ . Thereby, for  $1300\text{-}2700\text{ MHz}$  FMCW generation, the VCO is supplied by a periodic sawtooth signal of frequency  $f = 1\text{ KHz}$  and period  $T = 1\text{ msec}$ , minimum amplitude  $V_{min} = 0.15\text{ V}$ , and maximum amplitude  $V_{max} = 25\text{ V}$  as shown in Fig. 4. The corresponding FMCW signal will be repeated every period  $T$  as shown in Fig. 5. The generated FMCW signal is amplified by the (ZJL-5G) fixed gain power amplifier. The amplifier operating frequency range is from  $20\text{ MHz}$  to  $5\text{ GHz}$ . The amplifier maximum gain is  $9\text{ dB}$  with maximum output power of  $9.5\text{ dBm}$ . Finally the amplified FMCW signal is fed to the transmit horn antenna through a  $50\Omega$  coaxial cable.



**Figure 4:** The periodic sawtooth signal of period  $T = 1\text{ msec}$ , minimum amplitude  $V_{min} = 0.15\text{ V}$ , and maximum amplitude  $V_{max} = 25\text{ V}$ .

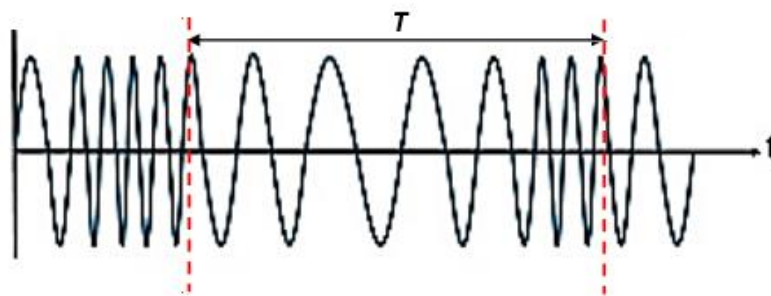


**Figure 5:** The FMCW signal that is repeated every period  $T$  of the designed sawtooth signal.

## 2.2 RFID Reader Receiver

At the receiving side, the received amplitude modulated FMCW at the receive horn antenna is passed through low pass filter (LPF) to remove the noise and unwanted high frequency components. The utilized LPF is the (SLP-2950+A) LPF with passband from DC to  $2700\text{ MHz}$  and maximum stopband attenuation of  $40\text{ dB}$ . The filtered signal is then amplified by the (ZJL-5G) fixed gain power amplifier and fed to the RF power detector.

The utilized RF power detector is the (ZX47- 60LN+) detector that converts the received RF signal into DC voltage. The power detector has input power dynamic range from  $-60\text{dBm}$  to  $+5\text{dBm}$  over operating frequency range from  $10\text{MHz}$  to  $8\text{GHz}$ . Generally, the RF power detector detects the RF signal power and generates a DC voltage signal whose amplitude is proportional to the received signal power. Accordingly, the RF power detector converts the received amplitude modulated FMCW into DC electrical voltage signal having constant amplitude with  $N$  discrete amplitude attenuations as shown in Fig. 6. Each amplitude hole corresponds to a binary bit “1” while the lack of hole corresponds to a binary “0”.

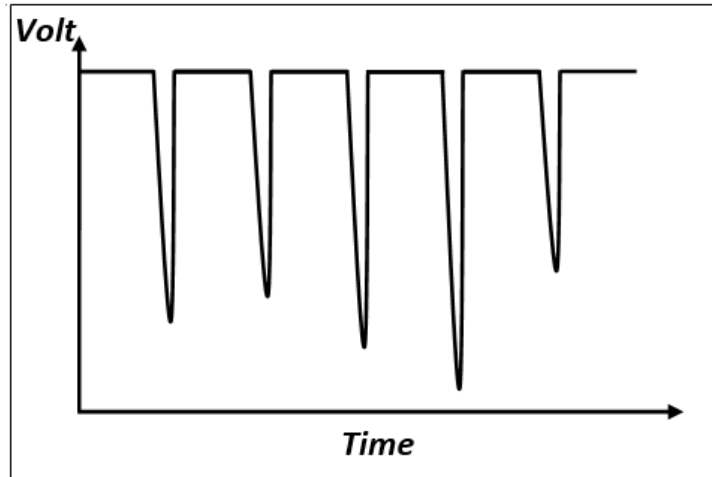


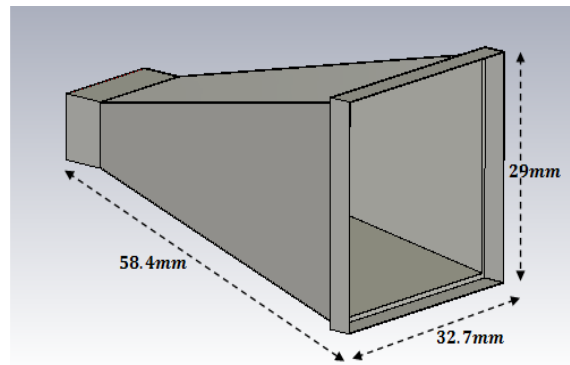
**Figure 6:** RF power detector output electrical voltage signal having constant amplitude with  $N$  discrete amplitude attenuations.

### 2.3 Control Unit and Monitoring System

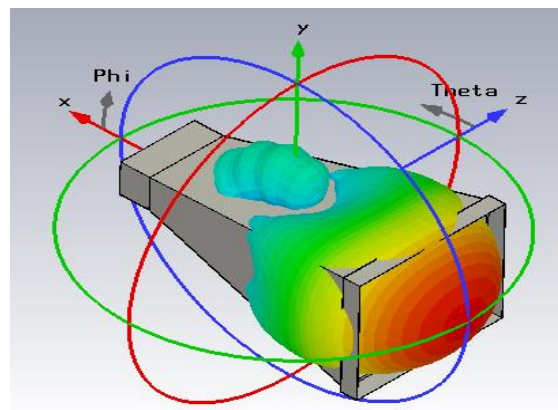
The main unit or the main brain of the RFID reader system is Arduino Uno. Arduino board is based on the ATME1519 which has all features of microcontrollers. It is simply connected to the computer using a USB cable which provides the required power to start the device operation and a mean for data transfer. The ATME16U2 is easily programmed using the USB cable and there is no need for a separate burner. The Arduino supplies the control voltages simultaneously to the sawtooth signal generator and the RF power detector for synchronized operation. The analog output signal from the RF power detector is converted into a digital signal using analog to digital converter (A/D) and fed to the microcontroller, which transfers it to the monitoring unit.

### 2.4 RFID ReaderTX/RX Horn Antenna

The transmit and receive antennas of the RFID reader are chosen as a wide band pyramidal horn antenna with dimensions  $(32.7 \times 29 \times 58.4)\text{mm}^3$  using the standard ATH1G18A waveguide as shown in Fig. 7 (a). Fig. 7 (b) shows the CST simulated 3-D radiation pattern of the horn antenna at the center frequency  $f_0 = 6\text{GHz}$ . The horn antenna has gain =  $12.3\text{dBi}$ , side lobe level SLL =  $-18.4\text{dB}$  and half power beamwidth (HPBW) which equal  $46.7^\circ$  and  $42.8^\circ$  in the E-plane and H-plane, respectively as shown in Fig. 8 (a) and Fig. 8 (b).

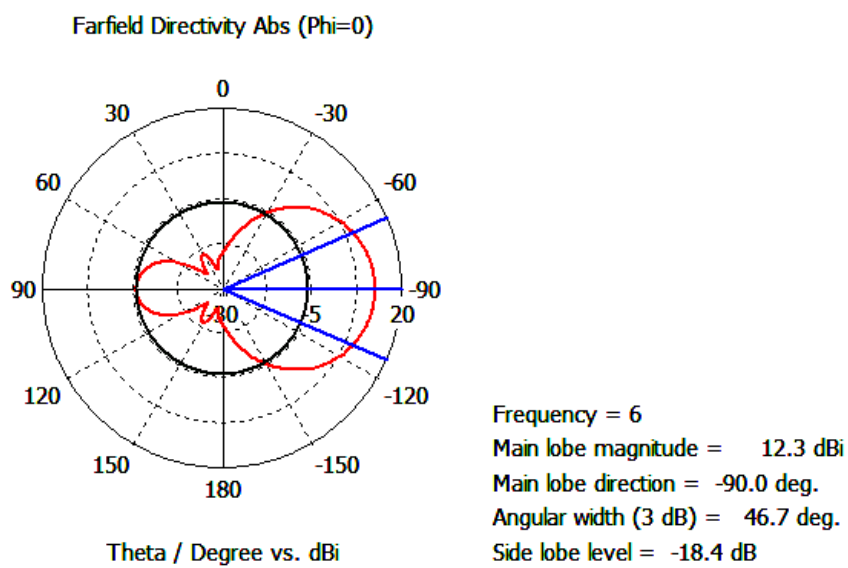


(a)



(b)

**Figure 7:** The geometry of the TX/RX horn antenna of the proposed RFID reader (a) geometry and (b) 3-D radiation pattern.



(a)

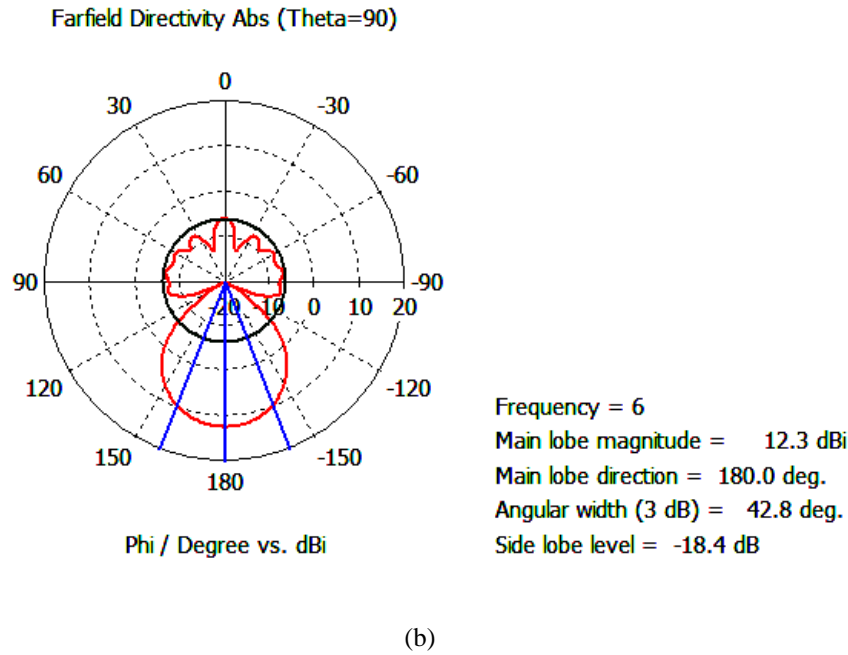


**Figure 8:** TX/RX horn antenna (a) E-plane radiation pattern at the center frequency  $f_0 = 6GHz$ , and (b) H-plane radiation pattern at the center frequency  $f_0 = 6GHz$ .

### 3. Hardware Implementation of The Proposed Chipless Tags

In this section, two chipless RFID tags with two binary ID codes, “11111” and “10101” are introduced. The general tag consists of five resonance circuits that are placed close to a  $50\Omega$  transmission line. Each resonance circuit has a unique resonance frequency that depends on its dimensions. The five resonance circuits are designed to resonate at the frequencies  $f_1 = 1.6 GHz$ ,  $f_2 = 1.8 GHz$ ,  $f_3 = 3 GHz$ ,  $f_4 = 2.2 GHz$ , and  $f_5 = 2.4 GHz$  respectively. The tags are printed on FR4 (lossy) substrate with relative permittivity  $\epsilon_r = 4.3$ , thickness  $h = 1.6 mm$ , and loss tangent  $\delta = 0.025$ .

#### 3.1 Design of general RFID tag for ID “11111”

The CST design of the general RFID tag is shown in Fig.9. The general tag is designed for ID “11111”. To change a binary “1” to a binary “0” at any resonance frequency, the corresponding resonance circuit is removed or short circuited. The dimensions of the general tag are declared in Fig. 10 and listed in Table (1). The simulated scattering parameter  $|S_{21}|$  of the general tag of binary code “11111” is shown in Fig. 11. The practical fabrication of the tag is shown in Fig. 12. The measured scattering parameter  $|S_{21}|$  of the fabricated tag using the Rohde & Schwarz ZVL20 Network Analyzer is shown in Fig. 13.



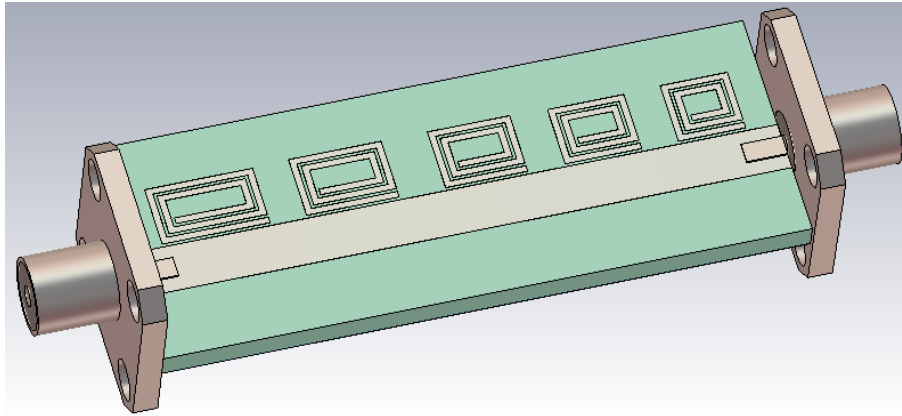


**Figure 9:** CST design of the general RFID tag of ID “11111”.

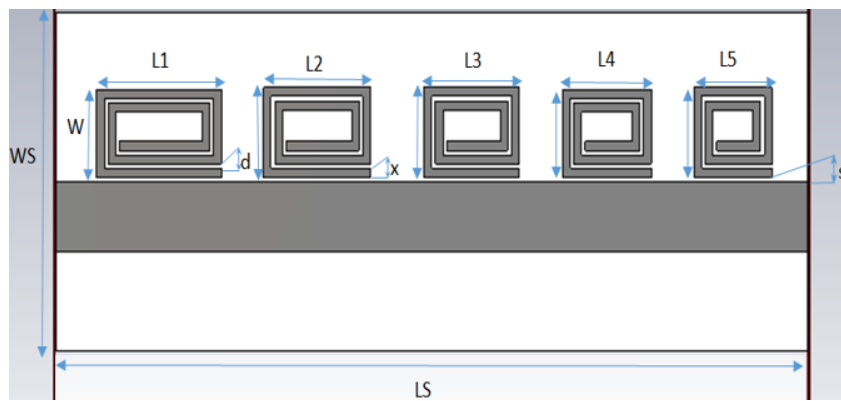


**Figure 10:** The dimensions of the general tag of ID “11111”.

**Table 1:** The dimensions of the general tag of ID “11111”.

Parameter	Dimension in (mm)
$L1$	6.6
$L2$	5.7
$L3$	5.05
$L4$	4.7
$L5$	4.15
$Ws$	15
$W$	4
$x$	0.4
$d$	0.2
$s$	0.1
$ls$	40

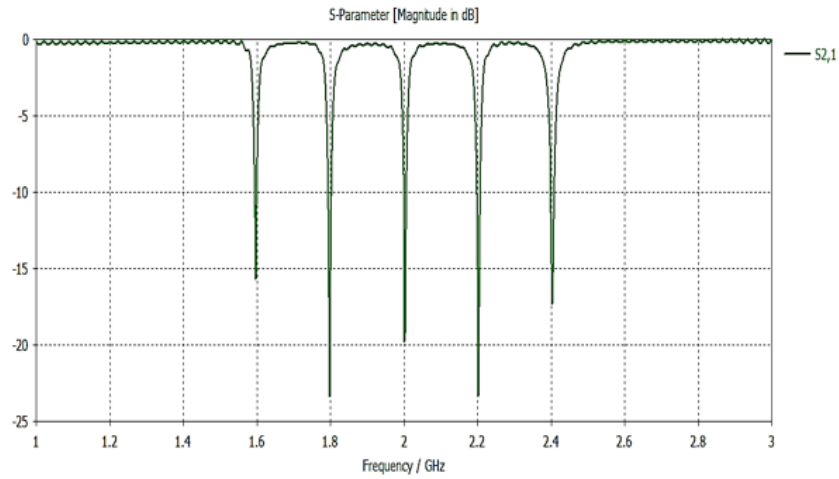


**Figure 11:** Simulated scattering parameter  $|S_{21}|$  of the general tag of binary ID code “11111”.

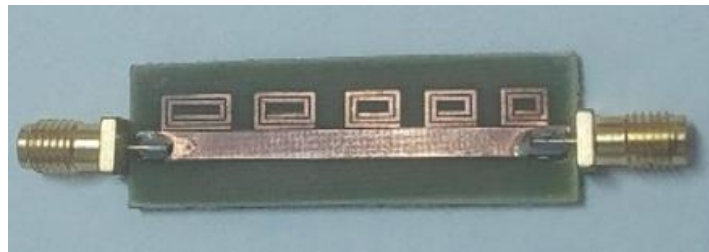


**Figure 12:** The practical fabrication of the general tag of binary ID code “11111”.

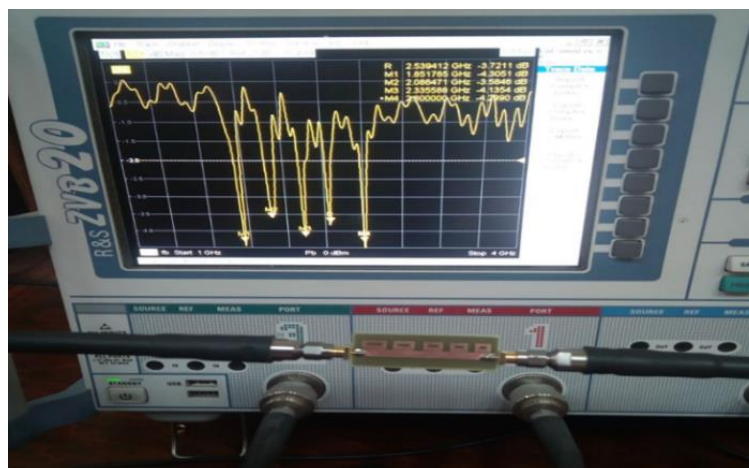


**Figure 13:** Measurement of scattering parameter  $|S_{21}|$  of the fabricated tag of binary ID code “11111”.

### 3.2 Design of RFID tag for ID “10101”

The CST design of the RFID tag for ID “10101” is shown in Fig.14. To implement binary “0” the second and fourth resonance circuits from the left side of the tag are short circuited as shown in Fig. 14. The simulated scattering parameter  $|S_{21}|$  of the tag is shown in Fig. 15. The practical fabrication of the tag is shown in Fig. 16. The measured scattering parameter  $|S_{21}|$  of the fabricated tag using the Rohde & Schwarz ZVL20 Network

Analyzer is shown in Fig. 17.

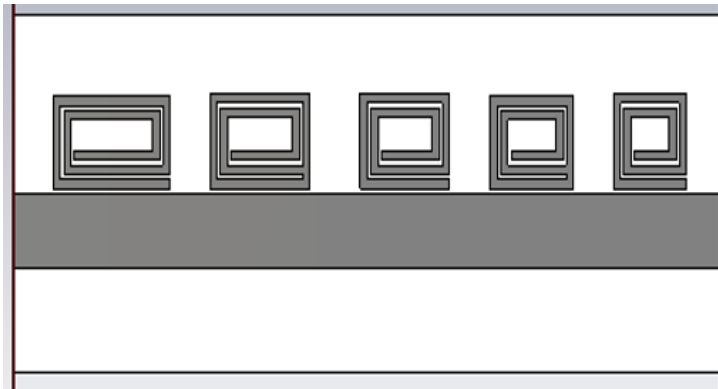


**Figure 14:** The CST design of the chipless tag that corresponds to binary code “10101”.

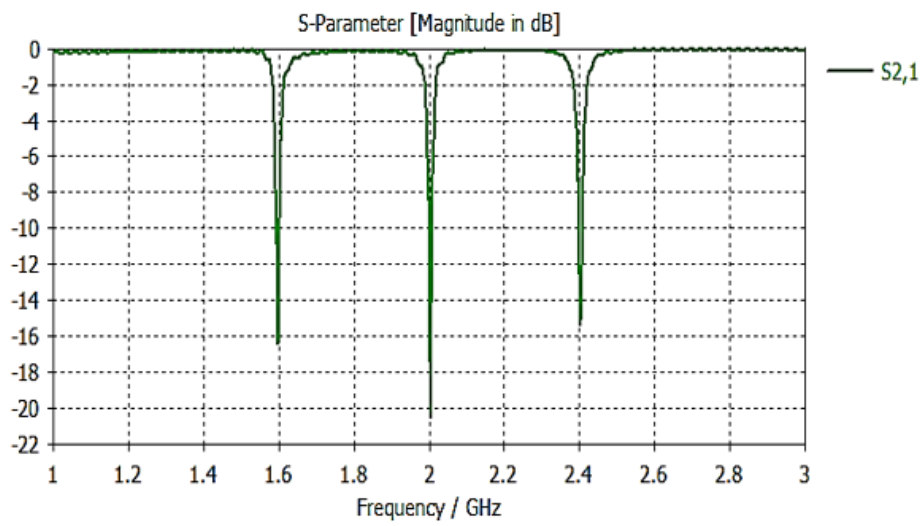


**Figure 15:** Simulated scattering parameter  $|S_{21}|$  of the tag of binary code “10101”.

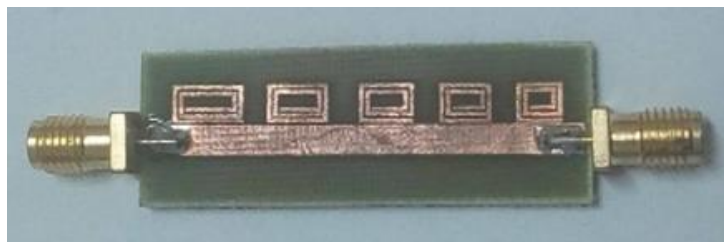


**Figure 16:** The practical fabrication of tag of “10101” binary code.

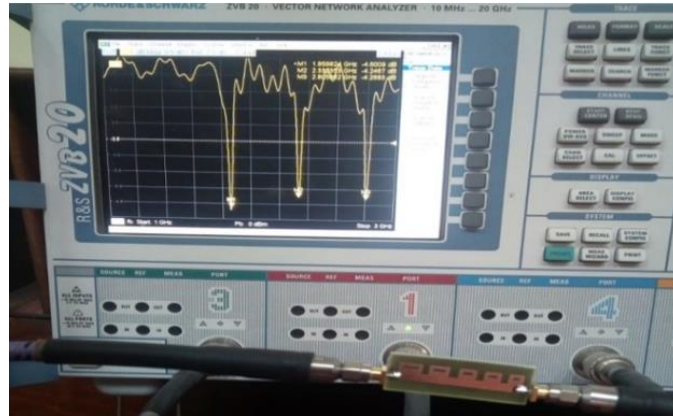


**Figure 17:** Measurement of scattering parameter  $|S_{21}|$  of the fabricated tag of binary ID code “10101”.

#### I. SIMULATION RESULTS OF THE ENTIRE RFID SYSTEM

In this section, the assembly of the proposed system components to form the entire RFID system is introduced as shown in Fig. 18. As it is difficult to obtain the two high gain horn antennas, the tag carrying binary ID “11111” is connected directly to the output of the reader transmit port and the reader receive port as shown in Fig 18. The RF signal is then passed through the tag that modulated the amplitude spectrum of the transmitted wide band signal. The measured scattering parameter  $s_{21}$  of the tag is shown in Fig. 19. It is clear that the RFID reader is succeeded to decode the 5-bits encoded code word.

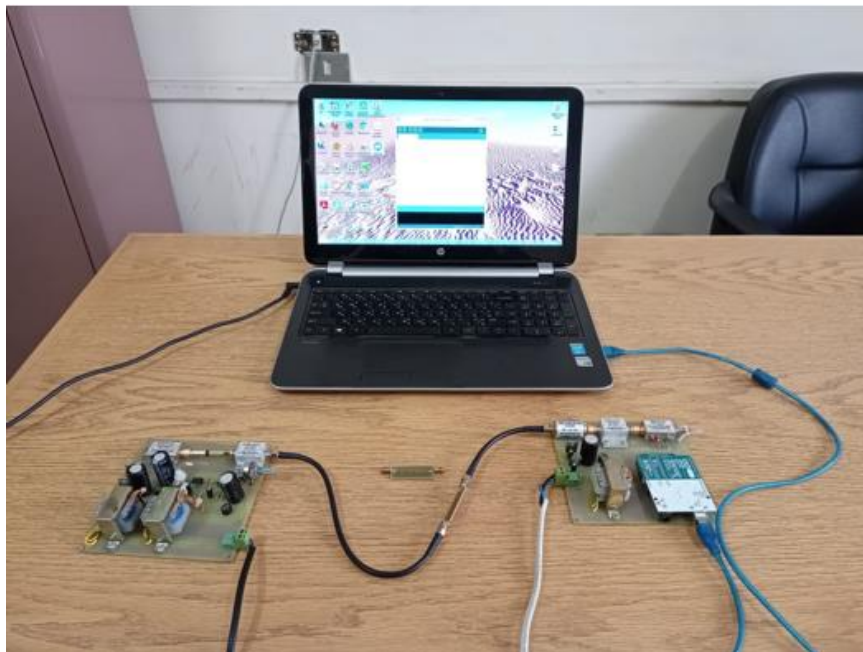


**Figure 18:** The assembly of the entire RFID system.

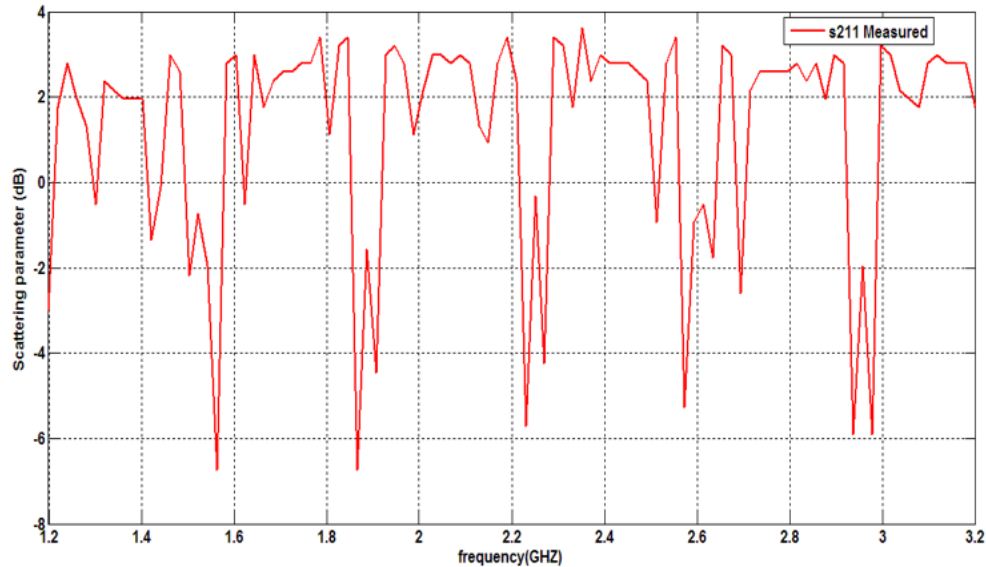


**Figure 19:** The measured  $s_{21}$  of the tag carrying binary ID “11111”.

#### 4. Conclusion

In this paper, the hardware implementation of a proposed RFID reader system for detecting wide varieties of chipless tags is introduced. For this purpose, the reader is supplied with tunable a wide band VCO and a wide band RF power detector with high sensitivity. The required electronic circuitry especially the sawtooth signal generator and control circuits are well designed and tested. In addition, we introduced a design and implementation of a 5-bits chipless tag for testing purposes. The simulation results of the tag are highly matched to the experimental measurements. When the entire system is assembled it is succeeded to decode the 5-bits encoded code word.

#### References

- [1] M. Sumi, R. Dinesh, C. M. Nijas, S. Mridula, and P. Mohanan, “High Bit Encoding Chipless RFID Tag Using Multiple E-Shaped Microstrip Resonators,” *Progress In Electromagnetics Research B*, Vol. 61, pp.185-196, 2014.
- [2] D. Girbau, J. Lorenzo, A. L´azaro, C. Ferrater, and R. Villarino, “Frequency-coded chipless RFID tag based on dual-band resonators,” *IEEE Antennas Wireless Propagation Letters*, Vol. 11, pp. 126–128, 2012.
- [3] M. S. Bhuiyan, and N. C. Karmakar, “An Efficient Coplanar Retransmission Type Chipless RFID Tag Based On Dual-Band MCSRR,” *Progress In Electromagnetics Research C*, Vol. 54, pp.133-141, 2014.
- [4] S. Preradovic, , I. Balbin, N. C. Karmakar, and G. F. Swiegers, “Multiresonator-based chipless RFID system for low-cost item tracking,” *IEEE Transactions on Microwave Theory and Techniques*, Vol. 57, pp. 1411–1419, 2009.

- [5] M. A. Islam, Y. Yap, N. C. Karmakar, and A. Azad, "Compact printable orientation independent chipless RFID tag," *Progress In Electromagnetics Research C*, Vol. 33, pp. 55–66, 2012.
- [6] A. Vena, E. Perret, and S. Tedjini, "High capacity chipless RFID tag insensitive to the polarization," *IEEE Trans. Antennas Propag.*, Vol. 60, No. 10, pp. 4509–4515, 2012.
- [7] C. M. Nijas , R. Dinesh, U. Deepak, A. Rasheed, S. Mridula, K. Vasudevan, and P. Mohanan, "Chipless RFID tag using multiple microstrip open stub resonators," *IEEE Trans. Antennas Propag.*, Vol. 60, No. 9, pp. 4429–4432, 2012.
- [8] A. Chatterjee, S. Manna, A. Rahaman, A. R. Sarkar, A. Ghosh and A. A. Ansari, "An Automated RFID Based Car Parking System," 2019 International Conference on Opto-Electronics and Applied Optics (Optronix), Kolkata, India, pp. 1-3, 2019.
- [9] Y. Zhang, Y. Ma, K. Liu, J. Wang and S. Li, "RFID based Vehicular Localization for Intelligent Transportation Systems," 2019 IEEE International Conference on RFID Technology and Applications (RFID-TA), Pisa, Italy, pp. 267-272, 2019.